Surface Based Modeling of Ground Motion Areas in Lower Saxony

Bahareh Mohammadivojdan, Hamza Alkhatib,
Marco Brockmeyer, Cord-Hinrich Jahn & Ingo Neumann

Systematic investigations have shown subsidence in almost 30% of the land area in Lower Saxony. It is essential to model these variations of the Earth surface especially to update the spatial reference system. Since the geodetic observations result in discrete points, it is necessary to mathematically model these measurements to have a continues surface. This enables the user to do predictions at any position. This is challenging especially because these types of measurements usually result in non-uniformly distributed data. There are different approaches to deal with this problem, here the stochastic method of Kriging and the deterministic method of Multilevel B-Splines are implemented to model ground motion.
This paper investigates the ground motion of specific areas in Lower Saxony through the cooperation of Landesamt für Geoinformation und Landesvermessung Niedersachsen (LGLN) and Geodetic Institute of Hannover. For this investigation, a time series of measurements from leveling, Global Navigation Satellite System (GNSS) observations and height changes that are acquired by Persistent Scatterer Interferometry (PSI) technique are taken into consideration. Evaluation of the results show not only good performance and promising results from both the approaches, but also compatibility between the approximated surface from both of them.
keywords: Ground motion in Lower Saxony, Multilevel B-Splines, Kriging, Surface Approximation

1. Introduction

To provide a uniform, integrated spatial reference system, it is essential to have an up-to-date benchmark network. Due to variations of the Earth surface, the official spatial reference system differs from the current calculated coordinates. It is important to determine these variations and model the ground movements to be able to update the spatial reference system. This is not an easy task since all geodetic measurement techniques will result in discrete points. Also, these measurements are mostly non-uniformly distributed and contain data gaps. Therefore it is necessary to mathematically model the data set to have a continuous surface. This enables the user to obtain the target quantity at any position and to predict in areas where fewer observations are available.
A data set contains both deterministic and stochastic parts. For accurately modeling the underlying function of the data, different methods should be taken into account to deal with both parts of each data set. There are several known deterministic and stochastic approaches to deal with the problem of surface approximation. Among the deterministic

approaches, traditional polynomial surface and free-form surfaces, such as Bézier, B-Splines, and Non-uniform rational B-Splines could be mentioned NURBS. Least Squares Collocation (Straub 1996), Gaussian Processes (Rassmussen & Williams 2006) and Kriging (Montero et al. 2015) are examples of stochastic approaches.
Deterministic approaches mainly model the trend part of the data set. Whereas stochastic methods deal with the stochastic properties. Stochastic methods are based on spatial or temporal correlation between data points and use a covariance function or a variogram to describe such relations. Both deterministic and stochastic approaches provide optimal solutions based on the complexity of the data set and individual applications. For more information the reader is referred to (Schabenberger & Gotway 2017).
A common approach for surface approximation is the method of Kriging. It should be noted that in a stochastic method such as Kriging, an assumption is that the data set is homogeneous. Therefore to get reliable results, the trend in the data should be removed. Another assumption is the existence of spatial correlation among the data points which means that neighboring points behave similarly that may not always be the case. Therefore, a method with less such limitations and more computational efficiency might be more appropriate for some applications. B-Splines is a proper alternative to Kriging which has less complexities yet delivering optimized results. Detailed description of these methods and results of their application on real data set are provided in the following sections.
Using the two methods of Kriging and Multilevel B-Splines Approximation (MBA), the ground movement in the area of Hengstlage is modeled. A continuous velocity field based on non-uniformly distributed measurements of height changes and horizontal displacements of the Earth surface is estimated by both methods. In particular height components which are acquired by PSI data in combination with leveling data are analyzed.
This paper is organized as follows. Section 2. reviews the main ideas behind the two approaches of Kriging and MBA. In section 3. the results related to validation and comparison of the analysis of the mentioned methods through applying a closed-loop Monte Carlo (MC) simulation including cross-validation on an exemplary reference data is presented. Section 4. contains the results of applying these approaches to real data sets related to ground movement in the area of Hengstlage.

2. Scattered data approximation

Approximation of scattered data refers to the problem of fitting a surface through a set of non-homogeneously distributed data points which is a common problem in different fields of studies. The main goal is to find the underlying function as a surface, which best describes the behavior of the data and makes it possible to propagate the existing information from the positions where measurements are available to new positions where no data exist. Let (x, y) present an arbitrary position, we look for the function $f(x, y)$ which computes the z value at that position.

$$z = f(x, y) \tag{1}$$

2.1. Approximation with Kriging

Kriging is a geostatistical approach which is based on the assumption that there is a spatial correlation among the data set. This method results in a prediction surface and performs prediction by summing the weighted observations around the desired location. The prediction in Kriging is done by means of Eq. 2 using a linear combination of the observations (z_i) and their weights (λ_i) (Montero et al. 2015). In this equation, (x_0, y_0) represents a point where prediction is desired.

$$z^*(x_0, y_0) = \sum_{i=1}^{n} \lambda_i z_i, \tag{2}$$

The weights $\{\lambda_1, \lambda_2, ..., \lambda_n\}$ are calculated using a semivariogram. A semivariogram is a variance function which represents the dissimilarities between the data points. In order to derive the semivariogram the first step is calculating an experimental semivariogram based on the observations (see Eq.3, (Montero et al. 2015)). To derive this semivariogram, it is important for the data to be stationary. The experimental semivariogram values ($\hat{\gamma}(h)$), which show the variability of the data points at different distances, are calculated considering predefined lags (h). Lags are the distances in which the semivariogram is calculated. In Eq. 3, $N(h)$ represents the number of observation pairs within the lag distance.

$$\hat{\gamma}(h) = \frac{1}{2N(h)} \sum_{n=1}^{N(h)} (z_n - z_{n+h})^2 \tag{3}$$

The next step is fitting a theoretical semivariogram (γ) to the discrete function (Eq. 3). Weights for prediction in position (x_0, y_0) can be calculated by solving the following equation for all the observations simultaneously (Montero et al. 2015). In Eq. 4 $\gamma((x_i, y_i) - (x_j, y_j))$ is the semivariogram value corresponding to the observation location pairs (x_i, y_i) and (x_j, y_j) and $\gamma((x_i, y_i) - (x_0, y_0))$ is related to semivariogram values relative to the prediction location.

$$\sum_{j=1}^{n} \lambda_j \gamma((x_i, y_i) - (x_j, y_j)) = \gamma((x_i, y_i) - (x_0, y_0)) \tag{4}$$

It should be noted that in a stochastic method such as Kriging, the basic assumption is the homogeneity of the data. In other words, in order to get reliable results, the trend in the data should be removed in advance.

2.2. Approximation with Multilevel B-Splines

Multilevel B-Splines for scattered data is an approximation method based on hierarchical tensor product B-Splines surfaces. The method was first developed in the 1990s for specific image processing applications such as image morphing (Lee et al. 1995). Lee

et al. (1997) introduced a modified version of this method for general scattered data approximation tasks.

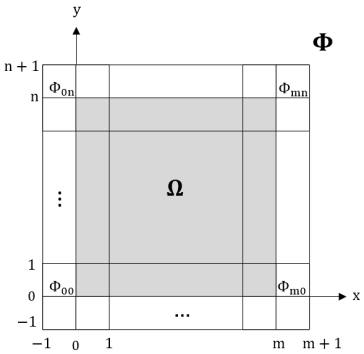

Figure 1: Configuration of control lattice Φ (Lee et al. 1997).

The B-Spline surface is defined by a control lattice Φ overlaid on the domain Ω. Where $\Omega = \{(x, y)|0 \leq x < m, 0 \leq y < n\}$ is a rectangular domain defined in xy plane containing all the observations. The control lattice Φ is an $(m + 3) \times (n + 3)$ lattice which overlaps the integer values of Ω. In which ϕ_{ij} is the value of the ij-th control point on lattice $\mathbf{\Phi}$, for $i = -1, 0, \ldots, m + 1$ and $j = -1, 0, \ldots, n + 1$ (Figure 1).
The B-Splines surface f is linear combination of uniform bicubic basis functions ($B_k(s)$, $B_l(t)$) and control points of a control lattice $\mathbf{\Phi}$, where $i = \lfloor x \rfloor - 1, j = \lfloor y \rfloor - 1, s = x - \lfloor x \rfloor, t = y - \lfloor y \rfloor$.

$$f(x, y) = \sum_{k=0}^{3} \sum_{l=0}^{3} B_k(s) B_l(t) \phi_{(i+k)(j+l)} \tag{5}$$

The uniform cubic basis functions $B_k(s)$ for $0 \leq t < 1$, are defined as follows,

$$\begin{aligned} B_0(s) &= \frac{(1 - s)^3}{6}, \\ B_1(s) &= \frac{(3s^3 - 6s^2 + 4)}{6}, \\ B_2(s) &= \frac{(-3s^3 + 3s^2 + 3s + 1)}{6}, \\ B_3(s) &= \frac{t^3}{6}. \end{aligned} \tag{6}$$

Similarly, the basis functions $B_l(t)$ are calculated. In the estimation of the control points, all the data points that lie within the 4×4 neighborhood of that control point affect the

solution. From each point P_c in the neighborhood of a control point, one solution can be derived ϕ_c. The unique solution ϕ_{ij} for a control point is derived from minimization of error term $(w_c\phi_{ij} - w_c\phi_c)$ for all points. Where $w_c = B_k(s)B_l(t)$, $k = (i+1) - \lfloor x_c \rfloor$, $l = (j+1) - \lfloor y_c \rfloor$, $s = x_c - \lfloor x_c \rfloor$, $t = y_c - \lfloor y_c \rfloor$. The minimization could be solved through a Gauss Markov Model. And the final solution is as follows (Lee et al. 1997):

$$\phi_{ij} = \frac{\sum_c w_c^2 \phi_c}{\sum_c w_c^2}. \tag{7}$$

MBA algorithm by Lee et al. (1997) uses a hierarchy of control lattices to generate a sequence of f_k. The sum of all B-Spline surfaces in the hierarchy approximates the final desired surface. The approximation starts with a rough approximation and the resolution of the control lattices increase in each step. For approximation in using MBA, at first step, a hierarchy of control lattices $\mathbf{\Phi}_0$, $\mathbf{\Phi}_1$, ..., $\mathbf{\Phi}_h$ are defined. The refinement here is in a way that from one lattice to the next, the spacing of the grid lines is halved. The first control lattice $\mathbf{\Phi}_0$ and the number levels of estimation h are parameters that should be fixed beforehand. The levels of refinement can be chosen based on approximation error. The MBA algorithm starts with the coarsest control point lattice ($\mathbf{\Phi}_0$). Then using the deviation of the estimated function to the original observations $\Delta^1 z$ based on ($\mathbf{\Phi}_0$), the control lattice of the next level is estimated. This process will continue until the last control lattice is estimated. In general at each level k, for estimation of the control lattices, the function f_k is calculated based on $\Delta^k z$.

$$\Delta^k z = z - \sum_{i=0}^{k-1} f_i(x,y) = \Delta^{k-1} z - f_{k-1}(x,y) \tag{8}$$

$$\Delta^0 z = 0 \tag{9}$$

The final approximation function is defined as the sum of functions in the hierarchy $f(x,y) = \sum_{i=0}^{k-1} f_i(x,y)$. An example of the process is illustrated in Figure 2 for a test data. In this figure, on the left side the original data set is shown and in the middle the control lattice hierarchy and the approximated functions at each level based on the related control lattice are illustrated. The 3D view of the approximated functions show how the estimation levels get refined in each step sequentially.

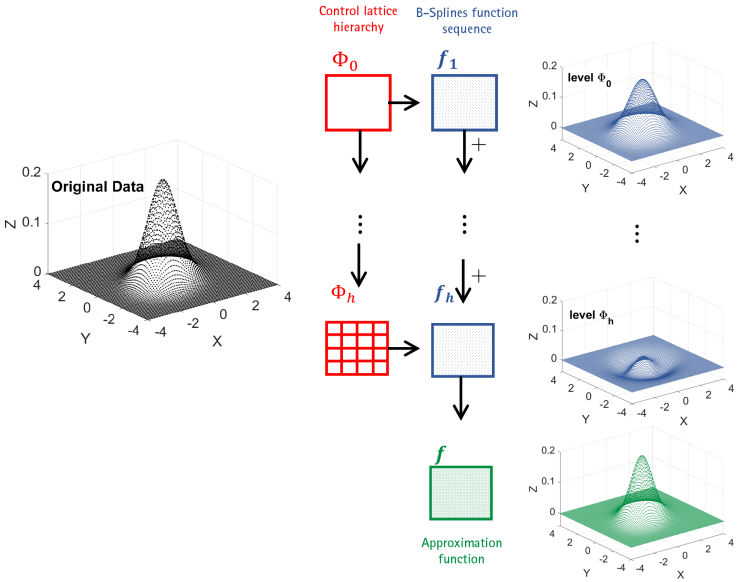

Figure 2: Schematic example of MBA approximation.

3. Validation of the methods

Before applying the mentioned surface approximation methods to a real data set, it is important to assess the functionality and performance of the methods to evaluate whether or not its results could be relied on in real applications. In this context, the reliability of the result is referred to as the approximation accuracy. In order to be able to judge such characteristics through a validation process, the true underlying function in a data set should be known beforehand. A 'segmented cross-validation' (Esbensen et al. 2010) method is implemented to assess the performance of the approximation methods individually and at the end a comparison between performances of the approaches is possible.
For this purpose, a reference data set is simulated and the details are explained in section 3.1.. The cross-validation is integrated into a MC simulation to include the effect of different realizations of the simulated data set in the validation process (section 3.2.).

3.1. Test data

The simulated data set for the cross-validation process is a 3D data set. Only z component of the data set is stochastic, x and y components are assumed to be deterministic.

The data set includes 6561 data points. The simulated data set can be split into two parts; the deterministic part or trend and the stochastic part or noise. The trend part of the 3D data set is generated by means of a multivariate Gaussian probability distribution function (PDF). The PDF is a mixture of two Gaussian distributions with the mean ($\boldsymbol{\mu}$) and variance-covariance matrix ($\boldsymbol{\Sigma}$) in accordance with Eq. 10. The x and y locations are equally distanced on a 0.1 grid where $-4 \leq x, y \leq 4$. The trend is constant over the full simulation:

$$\boldsymbol{z} \sim \mathcal{N}(0.6\boldsymbol{\mu}_1 + 0.4\boldsymbol{\mu}_2,\, \boldsymbol{\Sigma}_{11} + \boldsymbol{\Sigma}_{22}), \tag{10}$$

wherein:

$$\boldsymbol{\mu}_1 = \begin{bmatrix} 0.5 \\ 1 \end{bmatrix}, \quad \boldsymbol{\mu}_2 = \begin{bmatrix} -0.5 \\ -1 \end{bmatrix}, \tag{11}$$

$$\boldsymbol{\Sigma}_{11} = \begin{bmatrix} 2 & 0.5 \\ 0.5 & 0.5 \end{bmatrix}, \quad \boldsymbol{\Sigma}_{22} = \begin{bmatrix} 1 & 0.8 \\ 0.8 & 1 \end{bmatrix}. \tag{12}$$

The result can be seen in Figure 3a.

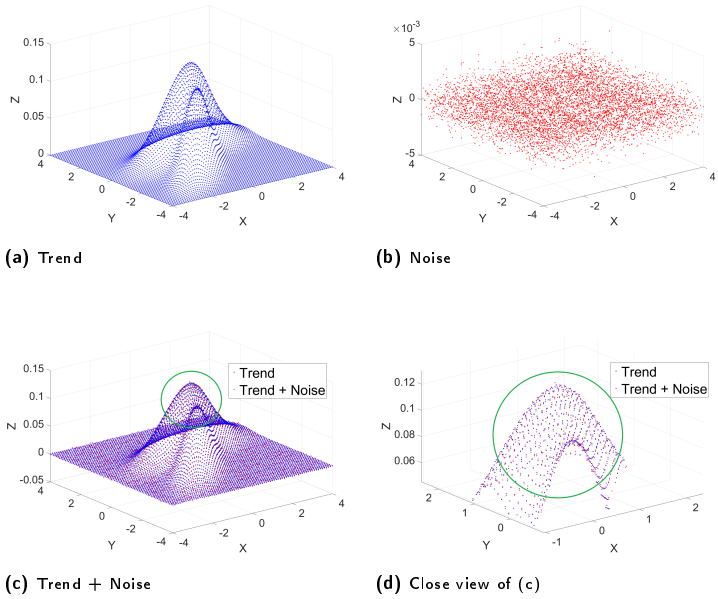

(a) Trend **(b)** Noise

(c) Trend + Noise **(d)** Close view of (c)

Figure 3: Separate visualizations of generated trend and noise.

The noise is generated from a Gaussian distribution with zero mean and standard deviation equal to 0.001.

$$noise \sim \mathcal{N}(0,\, 0.001^2) \tag{13}$$

The simulated data set is the combination of the deterministic trend and the stochastic noise. Figure 3 illustrates both parts separately. The combination of the two part is the input for the cross-validation process. For every MC run a new noise is simulated and added to the trend. Figure 3 only depicts one example for such a process.

3.2. Cross validation and Monte Carlo simulation

In segmented cross-validation for each iteration, q% of the whole data set is selected and eliminated as the test data set. The remaining part, or so-called training data set, is introduced to the surface approximation method to estimate the underlying function in the data set. Then the approximation method predicts the function values in the position of the test data. Since the true values of the test data are known, at the end the differences between the prediction (z^*) and the true value of the test data are used to assess the performance of the method. Here Root Mean Square Error (RMSE) of the differences, in accordance with Eq. 14, is used as a measure for the prediction error (Martens & Martens 2001).

$$RMSE = \sqrt{\frac{1}{n}\sum_{i=1}^{n}(z_i - z_i^*)^2} \tag{14}$$

However, cross-validation only on one data set will not guarantee the functionality of the methods. To ensure their performance, they should be subjected to different data sets. In this case, through a certain number of MC runs, the cross-validation is repeated for different realizations of the simulated data set. In each realization, a different noise is generated. The general algorithm of the implemented MC simulation environment is outlined in Algorithm 1. Here the number of MC runs (k_2) is set to 500 and the number of cross-validation iterations k_1 is set to 100. The results of the MC simulations are provided in the next section.

Algorithm 1: Monte Carlo Simulation.

Input: trend part of data set $\mathbf{Q}_{[n\times 3]} = [\mathbf{x} \quad \mathbf{y} \quad \mathbf{z}]$ generated from Eq. 10
Output: prediction for removed observations, RMSE of cross validations, mean of RMSEs
for $i = 1 \rightarrow k_2$ **do**
  generate noise vector ($\mathbf{noise}_{[n\times 1]}$) from Eq. 13
  set $\mathbf{P}_{[n\times 3]} = \mathbf{Q}_{[n\times 3]} + \mathbf{noise}_{[n\times 1]}$
  for *all surface approximation methods (Kriging and MBA)* **do**
    for $j = 1 \rightarrow k_1$ **do**
      remove m points (q%) from $\mathbf{P}$
      test data set ($\mathbf{P}''$) = the removed m data points
      training data set ($\mathbf{P}'$)= data set $\mathbf{P}$ after removing test data $\mathbf{P}''$
      model estimation based on $\mathbf{P}'$
      for $k = 1 \rightarrow m$ **do**
        prediction in $P''_k = (x_k, y_k)$
      calculate RMSE (Eq. 14)
calculate mean of $k_1 \times k_2$ RMSEs

3.3. Simulation results

In the method of Kriging, an exponential function for a variogram is selected. The effective area for calculation of the weights is considered to be the whole field. In case of applying MBA on a data set, two parameters should be fixed beforehand; the number of control points in the coarsest control lattice $\mathbf{\Phi}_0$ and the number of levels in the control lattice hierarchy (h). Through a sensitivity analysis, $m_0 = n_0 = 5$ for the coarsest control lattice with three levels of refinement is selected as an optimal solution. For the evaluation of the aforementioned surface approximation methods, five MC simulations for different cross-validation parameters are applied. The size of the test data increases by 10% in each simulation to study the effect of data gaps on the performance of the methods. Overall, each simulation contains 500 MC runs and each run includes 100 cross-validation iterations. In each MC run, a new noise vector is generated. The noise is constant during the 100 iterations of cross-validation and only the combination of the test data changes.

The results of the performance of the methods are illustrated in Figure 4. In this figure, the horizontal axis represents different MC simulations based on the size of the test data. Larger test data results in larger data gaps in the training set. The vertical axis presents the mean of the RMSEs from all MC runs. The performance of Kriging and MBA throughout the simulations are relatively steady. MBA has a smaller prediction error in comparison to Kriging. By increasing the size of the data gaps the quality of approximation decreases and especially in the case of Kriging. It can be seen that the prediction error derived with respect to 'trend + noise' is in the range of the generated noise. This means that the methods are smoothly predicting the true trend in the data set. Overall, the results show that MBA has smaller prediction error and is the more robust against data gaps.

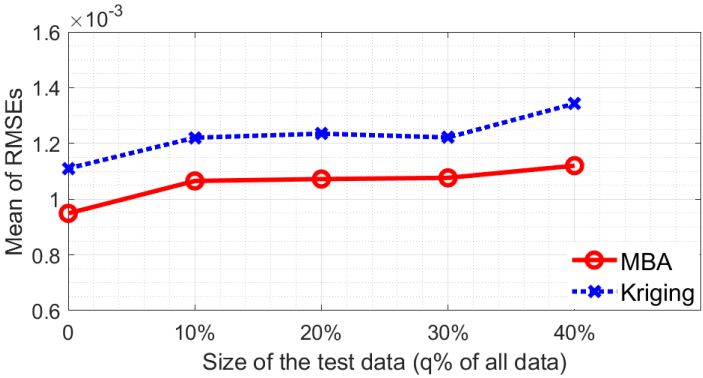

Figure 4: Mean of RMSEs for different MC simulations.

4. Ground motion in Hengstlage

Systematic investigations of different data sources in 2007 have shown that approximately 30% of Lower Saxony's land area is influenced by ground movements due to raw material extraction. These movements are due to the construction and operation of cavern facilities as well as the storage of CO_2 and hydrocarbons in the area (Jahn et al. 2011). This emphasized the necessity to update the official spatial reference system in the related area. Here specifically the ground movement in the area of Hengstlage is investigated. For this purpose, both the stochastic method of Kriging and the deterministic method of MBA are employed.

4.1. Data set

To investigate the ground movement, all measurements up to now are used as a basis to derive the related velocity information. In general, data from GNSS observations, leveling and PSI are used as a basis for the investigation of recent movements of the Earth's crust. For this purpose, the existing time series of vertical and horizontal benchmarks from 'amtlichen Festpunktinformationssystem' (AFIS) in Lower Saxony are gathered (Brockmeyer 2019).

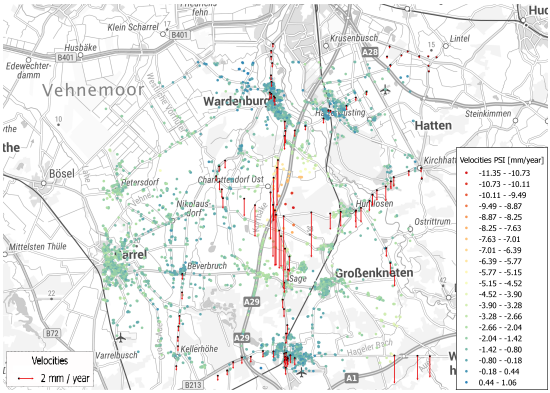

(a) Height component

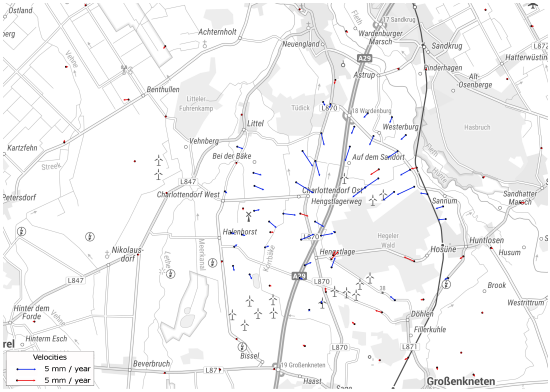

(b) Horizontal component

Figure 5: (a) PSI and leveling data (red bars), (b) Data from AFIS (red) and SA*POS*® (blue) in Hengstlage (Brockmeyer 2019).

Since 2008, a uniform coordinate monitoring by the satellite positioning service of the German national survey (SA*POS*®) reference stations has been continuously carried out in Lower Saxony for quality assurance of the SA*POS*® services. The results of these weekly GNSS evaluations are free coordinate solutions with complete stochastic information, which are examined in time series analysis to determine the three-dimensional motion behavior of the reference stations. Besides the regular data acquired from leveling and GNSS observations, vertical data which are acquired by the PSI technique, are also taken into consideration. Velocity information from PSI, as a part of the group of differential Interferometric Synthetic Aperture Radar (InSAR), plays an important factor in the ana-

lysis of ground movement due to the fact that this method provides denser information especially outside the regular geodetic networks and specifically in urban areas.
All the velocities, derived from different measurement methods, are considered to be uncorrelated. The variance related to vertical component derived from leveling and horizontal velocities are calculated based on Eq. 15. The variances are based on the accuracy of the individual measurements and time difference between measurements (α_t). The prior standard deviation (σ_0) in this case is considered to be 3 [mm] (Brockmeyer 2019).

$$\sigma^2 = 2\frac{1}{\alpha_t^2}\sigma_0^2 \tag{15}$$

The variance related to PSI velocities is derived following Eq. 16. It should be noted that the PSI observations are considered to be less accurate, the larger uncertainty is included as a parameter to the variance (Δ_{PSI}). Δ_{PSI} shows the instability of points and is considered to be 2 [mm] (Brockmeyer 2019).

$$\sigma^2 = 2\frac{1}{\alpha_t^2}\sigma_0^2 + \Delta_{PSI}^2 \tag{16}$$

The vertical data from leveling includes measurements from 20 years (1988 until 2008) related to 106 benchmarks. The maximum observed vertical deformation in the center is -9.9 [mm/year]. The PSI measurements are acquired between 2003 and 2010. The number of these observations after preprocessing is 5962. In Figure 5a the PSI data set and the leveling are shown. The two measurement techniques of leveling and InSAR show comparable observations. The horizontal velocities in this area are derived from 115 benchmarks. The measurements are performed in the time span of 1968 until 2010. In Figure 5b the horizontal velocities acquired from SA*POS*® measurements (blue arrows) and GNSS-post processing (red arrows) are shown.

4.2. Results of approximation

The approximated ground movement for both height changes and horizontal displacements are illustrated together in Figure 6. Height changes are presented as a heat diagram and horizontal displacements are specified as a vector field combining the displacement of the east and north components.
For approximation with MBA three levels of control lattice hierarchy in which the coarsest control lattice is $\mathbf{\Phi}_4$ ($m = n = 4$) are selected. Overall three control lattices $\mathbf{\Phi}_4$, $\mathbf{\Phi}_8$ and $\mathbf{\Phi}_{16}$ are used. Figure 6b shows the results of the estimation. The subsidence in the middle of the area is in both approximations distinguished.
For the approximation of horizontal displacement, observations of east and north components are analyzed separately. The methods of Kriging and MBA show similar results. For this analysis, similar specifications are used for the methods as in height changes approximation. The maximum absolute velocities in displacements appear around the edges of the subsided area. In the center of the subsidence area, horizontal displacement is zero.

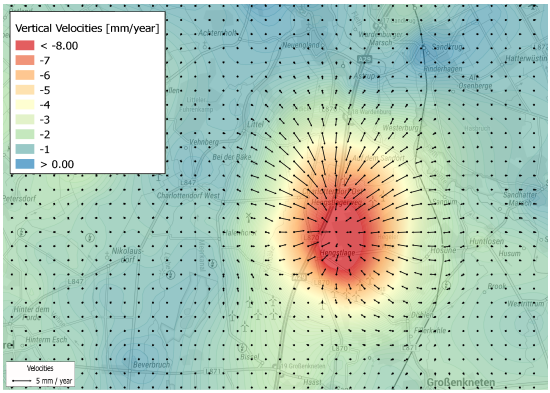

(a) Kriging

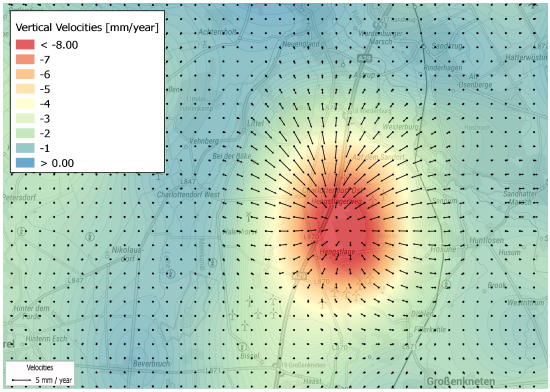

(b) MBA

Figure 6: Ground movement approximated by (a) Kriging (b) MBA (height changes are illustrated as heat diagram and vector field represents the horizontal displacements).

Figure 7 shows a 3D view of the approximated surface related to height changes by the two methods. The RMSE representing the prediction error in the location of the observations for Kriging and MBA are 0.44 and 0.47 [mm/year], respectively.
The approximations show similar behavior but they are not the same. The true function behind the ground movement is not known. To have a comparison between the result of these two approaches, the differences between the approximations are calculated.
Figure 8a shows a heat diagram of the absolute differences. Mostly the differences can be seen in areas where less observations are available. This results from different approaches of the two methods in interpolating information from positions with observations to data

gaps. The histogram of these differences in Figure 8b shows that they are randomly distributed overall the field.

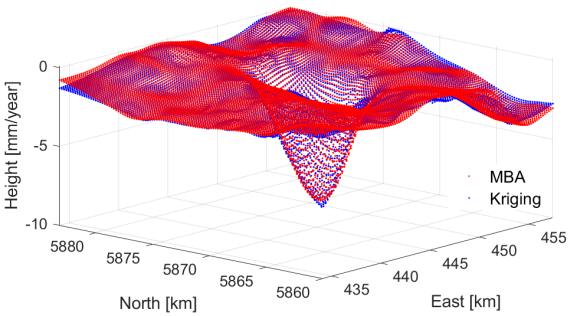

Figure 7: Approximation of the two methods of Kriging and MBA.

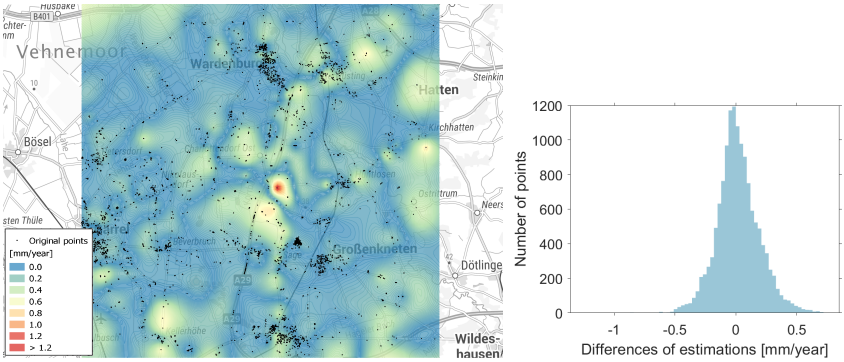

Figure 8: (a) Absolute differences (b) Histogram of the differences between approximation of Kriging and MBA.

5. Conclusion

In this paper, a stochastic and a deterministic surface approximation method are used to mathematically model ground movements. Specifically, the stochastic method of Kriging and a deterministic method based on B-Spline tensor product surfaces (MBA) are used. The performance and implementation of the methods are evaluated using cross-validation integrated into a closed-loop MC simulation. Different data sets are simulated, which

contain data gaps in order to be comparable to the real data set. Different appearances of data gaps in the simulated data help to investigate the effect of data gaps on the performance of the approaches. The results show that the quality of the estimation decreases by increasing the size of the data gaps. However, the method of MBA showed better performance in dealing with data gaps.
This research is a collaboration between LGLN and Geodetic Institute of Hannover. All the data set related to the ground movements in Lower Saxony are processed and provided by LGLN. The ground movement in the area of Hengstlage, modeled with the Kriging approach is implemented by LGLN. Height changes in this area are approximated with the two approaches and Kriging shows a smaller prediction error. The approximated surfaces by MBA and Kriging show a similar pattern of subsidence in the area and have comparable prediction errors. The Kriging method is computationally more expensive compared to the MBA. These results are also highly dependent on the used variogram and control lattice hierarchy.
For future research, it would be interesting to combine the deterministic and stochastic approaches. This means to estimate the trend in the data set by means of a deterministic method and model the remaining stochastic part with a stochastic method. In the method of MBA choosing an optimal control lattice hierarchy highly affects the final estimation. It is recommended to investigate an optimal control lattice hierarchy to obtain a more accurate estimation.

References

Brockmeyer, M. (2019): Daten der Landesvermessung zur räumlichen Interpolation von Bodenbewegungen. GeoMonitoring 2019, pp. 151 – 163, DOI: 10.15488/4519.

Chiles, J. & P. Delfiner (2009): Geostatistics: modeling spatial uncertainty. John Wiley & Sons, 497p.

Esbensen, K., Guyot, D., Westad, F. & L.P. Houmoller (2010): Multivariate Data Analysis - in practice. CAMO Software, Oslo.

Forsey, D. & P. Bartels (1992): Tensor products and hierarchical fitting. Curves and Surfaces in Computer Vision and Graphics II, V. 1610, pp. 88 – 96.

Forsey, D. & R. Bartels (1995): Surface fitting with hierarchical splines. ACM Transactions on Graphics, V. 14, pp. 134 – 161.

Jahn, C.-H., Feldmann-Westendorff, U., Grüer, D., Kulle, U. & P. Lembrecht (2011): Die Erneuerung des Deutschen Haupthöhennetzes in Niedersachsen. NaVKV, V. 4, pp. 3 – 7.

Lee, S. Y., Chwa, K.Y., Shin, S.Y. & G. Wolberg (1995): Image metamorphosis using snakes and free-form deformations. SIGGRAPH, V. 95, pp. 439 – 448.

Lee, S. Y., Wolberg, G., Chwa, K.Y. & S.Y. Shin (1995): Image metamorphosis with scattered feature constraints. IEEE Transactions on Visualization and Computer Graphics, V. 4, pp. 337 – 354.

Lee, S. Y., Wolberg, G., Chwa, K.Y. & S.Y.Shin (1997): Scattered data interpolation with multilevel B-splines. IEEE transactions on visualization and computer graphics, V. 3, pp. 228 – 244.

Martens, H. & M. Martens (2001): Multivariate analysis of quality. An introduction. IOP Publishing.

Montero, J.P., Delfiner, P. & J. Mateu (2015): Spatial and Spatio-Temporal Geostatistical Modeling and Kriging. John Wiley and Sons, United Kingdom.

Piegl, L. & W. Tiller (1997): The NURBS Book. Springer, Berlin.

Rassmussen C.E. & C.K. Williams (2006): Gaussian processes for machine learning. MIT press, Cambridge.

Schabenberger, O. & C. Gotway (2017): Statistical methods for spatial data analysis. Chapman and Hall-CRC.

Straub, C. (1996): Recent crustal deformation and strain accumulation in the Marmara Sea region, NW Anatolia, inferred from GPS measurements.PhD diss., ETH Zürich.

Contact

Bahareh Mohammadivojdan
Hamza Alkhatib
Ingo Neumann

Leibniz Universität Hannover
Geodätisches Institut
Nienburger Str. 1
30167 Hannover

Marco Brockmeyer
Cord-Hinrich Jahn

LGLN Landesvermessung und Geobasisinformation
Podbielskistraße 331
30659 Hannover